

Supporting Information

A POM-based copper-coordination polymer crystal material for phenolic compound degradation by immobilizing horseradish peroxidase

Ying Lu, Tong Zhang, Yue-Xian Zhang, Xiao-Jing Sang, Fang Su*, Zai-Ming Zhu*, Lan-Cui Zhang*

- 1. Selected bond lengths and angles of compounds 1 and 2**
- 2. The standard curves and H₂O₂ detection**
- 3. Synthesis and crystal structure figures**
- 4. Characterizations**
- 5. Enzyme immobilization and characterization**
- 6. Degradation of phenolic compounds by HRP/1**

1. Selected bond lengths and angles of compounds 1 and 2

Table S1 Selected bond lengths (Å) and angles (°) for compound 1

Bond	Length (Å)	Bond	Length (Å)	Bond	Length (Å)
Cu1–O21	1.878(12)	Cu2–N3	2.010(14)	P2–O23	1.534(14)
Cu1–O24	1.970(12)	Cu2–O22#2	2.250(13)	P2–O22	1.549(12)
Cu1–N2	1.996(15)	Cu3–O23	1.868(13)	P2–C31	1.807(18)
Cu1–N1	2.019(17)	Cu3–O26	1.899(12)	P3–O26	1.509(13)
Cu1–O24#1	2.401(12)	Cu3–N6	1.989(16)	P3–O24	1.518(13)
Cu2–O25	1.931(11)	Cu3–N5	1.998(15)	P3–O25	1.519(12)
Cu2–N4	1.978(17)	P2–O21	1.521(13)	P3–C41	1.827(17)
Cu2–O22	1.997(12)				
Bond	Angle (°)	Bond	Angle (°)	Bond	Angle (°)
O24–Cu1–N1	173.5(6)	O25–Cu2–O22	92.4(5)	O23–P2–C31	105.0(8)
N2–Cu1–N1	80.6(7)	O23–Cu3–N5	165.7(7)	O21–P2–C31	105.9(8)
O24–Cu1–O24#1	83.0(5)	N6–Cu3–N5	81.7(7)	O24–P3–O25	114.1(7)
O22–Cu2–N3	171.6(6)	O26–Cu3–N5	90.5(6)	O26–P3–C41	105.2(7)
N4–Cu2–N3	79.6(6)	O21–P2–O23	114.2(8)	O24–P3–C41	106.7(8)

Symmetry transformations used to generate equivalent atom

Table S2 Hydrogen bonds (Å, °) for compound 1

D–H···A	d(D–H)	d(H···A)	d(D···A)	<(DHA) (°)
O1W–H1WA...O4#1	0.851(10)	2.5(2)	2.98(3)	119(22)
O1W–H1WB...O18	0.851(10)	2.251(10)	3.01(3)	149(5)
O2W–H2WA...O2W#2	0.850(10)	2.150(10)	2.83(8)	137(11)
O2W–H2WB...O10	0.850(10)	2.53(15)	3.30(5)	152(28)

Symmetry transformations used to generate equivalent atoms: #1 -x+1, -y, -z; #2 -x, -y+1, -z

Table S3 Selected bond lengths (Å) and angles (°) for compound 2

Bond	Length (Å)	Bond	Length (Å)	Bond	Length (Å)
W1–O6	1.730(6)	W2–O1	1.961(6)	Cu1–O11	1.966(7)
W1–O3	1.826(7)	W2–O7#1	2.153(6)	Cu1–O1	1.972(6)
W1–O7	1.833(7)	W2–O8	2.243(6)	Cu1–N1	2.015(9)
W1–O8	1.969(6)	W3–O10	1.742(7)	Cu1–N2	2.031(8)
W1–O1	2.102(6)	W3–O4	1.807(7)	Cu1–O1w	2.285(8)
W1–O8#1	2.328(6)	W3–O11	1.812(7)	Cu2–O4#1	1.899(7)
W2–O9	1.738(7)	W3–O5#1	2.086(7)	Cu2–O2	1.907(7)
W2–O2	1.810(6)	W3–O3	2.104(6)	Cu2–N4	1.978(9)
W2–O5	1.879(7)	W3–O8#1	2.227(6)	Cu2–N3	1.993(9)
Bond	Angle (°)	Bond	Angle (°)	Bond	Angle (°)
O6–W1–O8#1	176.7(3)	O2–W2–O1	91.7(3)	O1–Cu1–N1	172.7(3)
O7–W1–O1	157.9(3)	O2–W2–O8	93.8(3)	N1–Cu1–N2	80.4(3)
O3–W1–O7	98.5(3)	O4–W3–O3	156.9(3)	O11–Cu1–O1	91.6(3)
O7–W1–O8	92.3(3)	O10–W3–O8#1	164.1(3)	O2–Cu2–N4	165.5(3)
O2–W2–O7#1	166.4(3)	O4–W3–O5#1	89.8(3)	N4–Cu2–N3	81.1(4)
O9–W2–O8	163.1(3)	O11–W3–O3	86.4(3)	O2–Cu2–N3	92.9(3)

Symmetry transformations used to generate equivalent atoms: #1 -x+2, -y+1, -z+1

2. The standard curves and H₂O₂ detection

(1) The standard curve of HRP

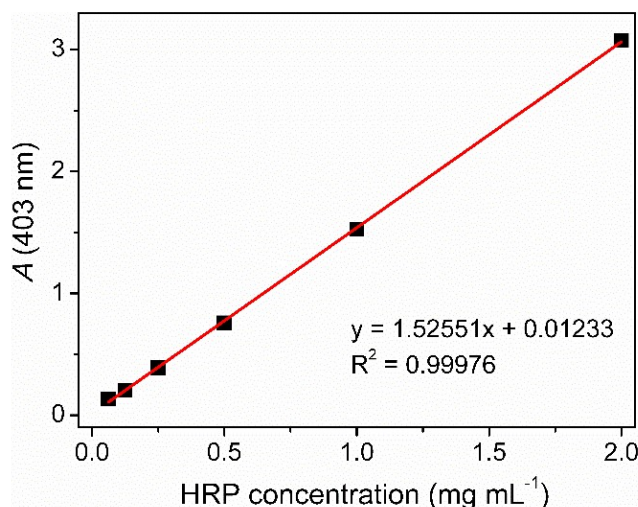


Fig. S1 The standard curve of HRP concentration versus absorbance (403 nm)

(2) The experiment of H₂O₂ detection

The experiment of H₂O₂ detection was performed as follows. 40 μ L of immobilized enzyme dispersion (pH 4.5, 5 mg mL⁻¹) was mixed with H₂O₂ solution (460 μ L, pH 4.5, 0.04–0.28 mmol L⁻¹) and 500 μ L of PBS (pH 4.5) containing 4 mmol L⁻¹ of 4-AAP and 1 mmol L⁻¹ of phenol. The resulting mixture was reacted for 2 min and centrifuged for 3 min at room temperature, and then the UV-vis absorption spectrum of supernatant was recorded at 510 nm.

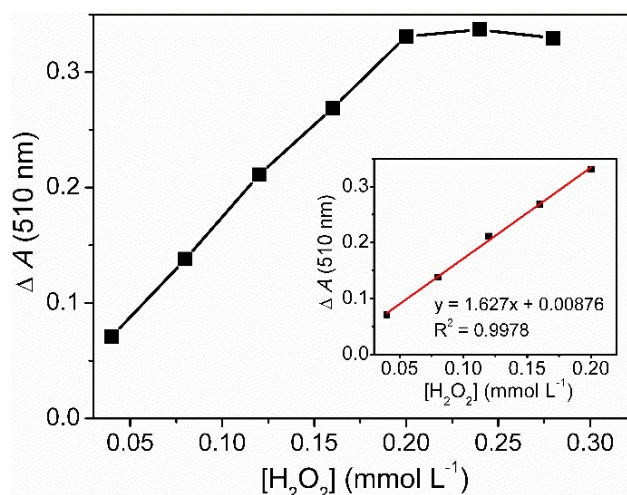


Fig. S2 The linear calibration plot for H₂O₂ detection using HRP/1 (HRP loading: 268 mg g⁻¹) as catalyst. $\Delta A = A$ (the immobilized HRP, 510 nm) – A (blank, 510 nm). The reaction time is 5 min

As shown in Fig. S2 (ESI†), the absorbance at 510 nm is increased with increasing the H₂O₂ concentration from 0.04 to 0.28 mmol L⁻¹. A linear relationship is observed between the absorbance and H₂O₂ concentration ranging from 0.04 to 0.20 mmol L⁻¹ catalyzed by HRP/1 with a detection limit of 3.06×10^{-3} mol L⁻¹. These results confirm that the activity of HRP is retained after immobilization on compound **1**, and HRP/1 is a kind of potential material for H₂O₂ detection.

(3) The standard curves of different phenolic compound

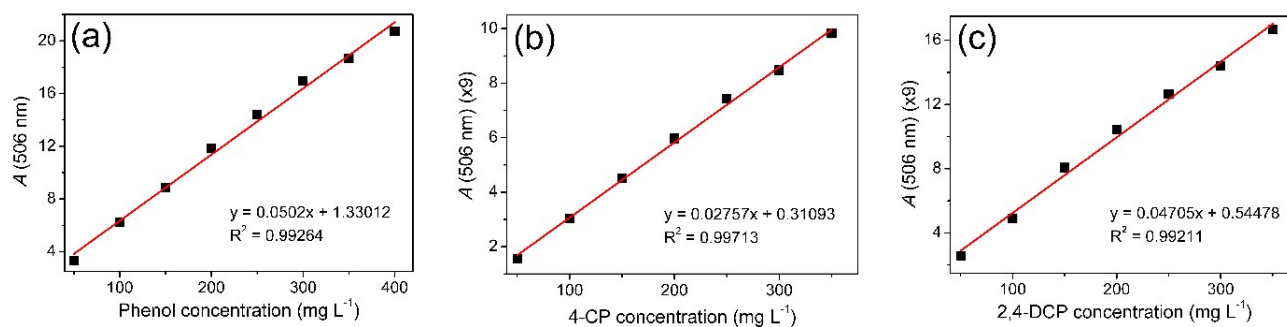
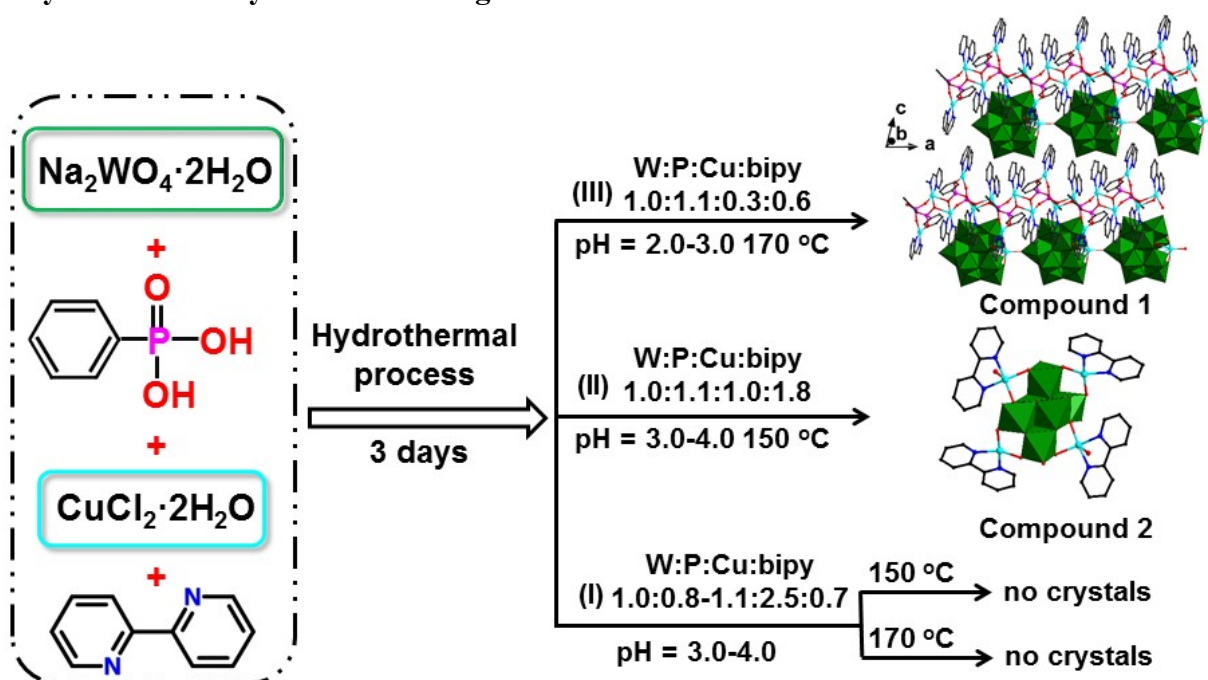


Fig. S3 The standard curves of (a) phenol, (b) 4-CP, (c) 2,4-DCP concentration versus absorbance (506 nm)

3. Synthesis and crystal structure figures



Scheme S1 Schematic representation of the synthetic pathway and conditions of compounds 1 and 2

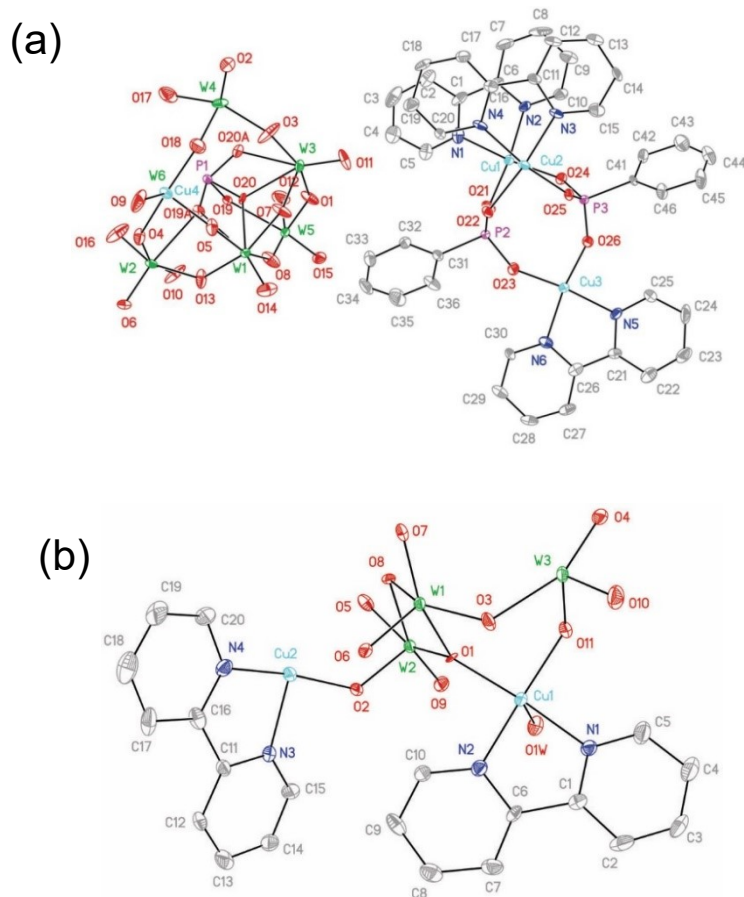


Fig. S4 (a, b) ORTEP view of the asymmetric unit of compounds **1** and **2** with atom labeling (30% probability displacement ellipsoids; hydrogen atoms and water molecules have been omitted for clarity)

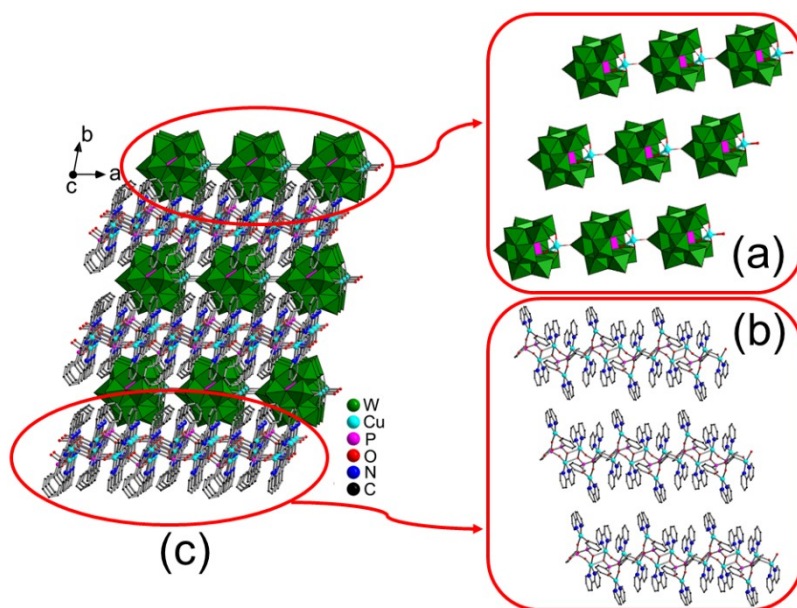


Fig. S5 (a, b) The arrangement of $[\text{PCuW}_{11}\text{O}_{39}]^{5-}$ polyoxoanions and $[\text{((Cu(bipy))}_2(\mu\text{-PhPO}_3)_2\text{Cu(bipy))}_2]^{4+}$ cations, respectively; (c) the packing view of an infinite 3D network of compound **1**

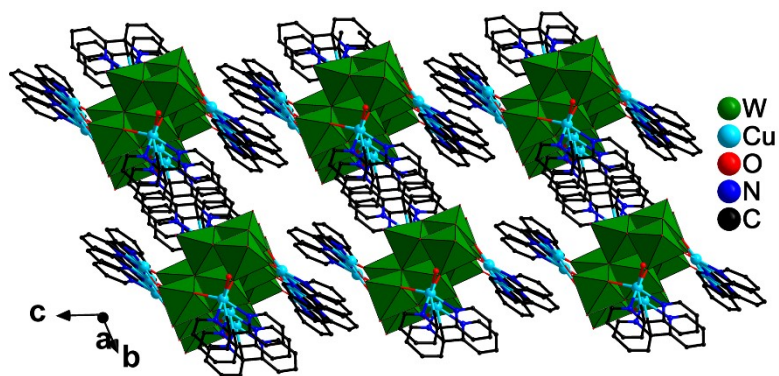


Fig. S6 3D packing diagram of compound 2

4. Characterizations

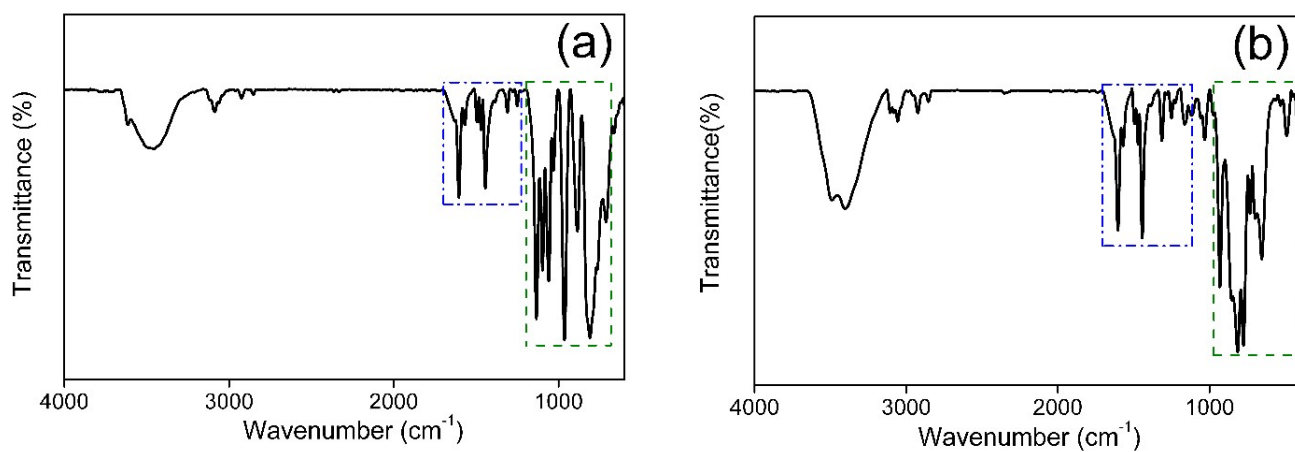


Fig. S7 (a, b) FTIR spectra of compounds 1 and 2

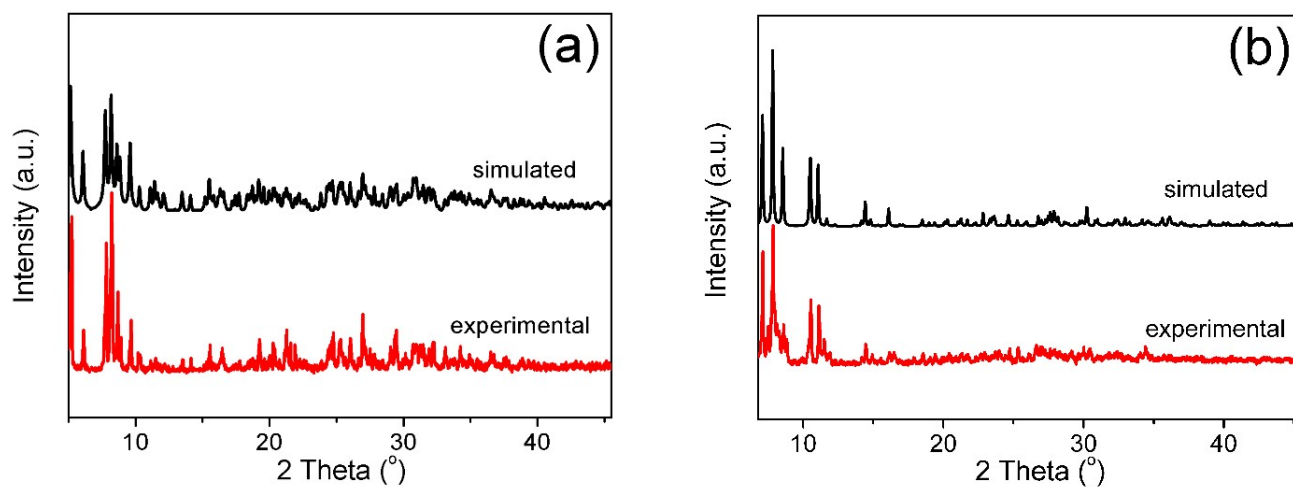


Fig. S8 (a, b) The simulated and experimental PXRD patterns of compounds 1 and 2

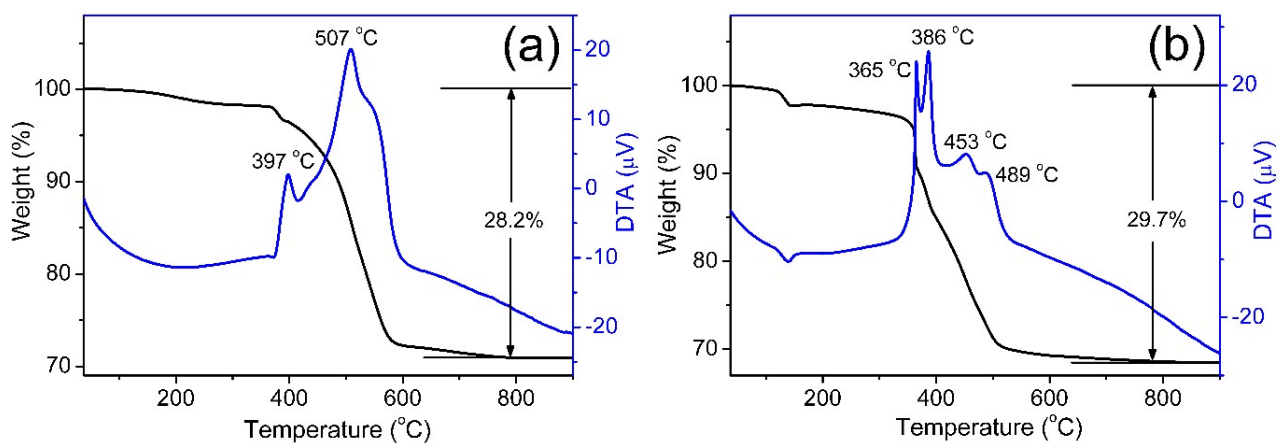


Fig. S9 (a, b) TG-DTA curves of compounds **1** and **2**

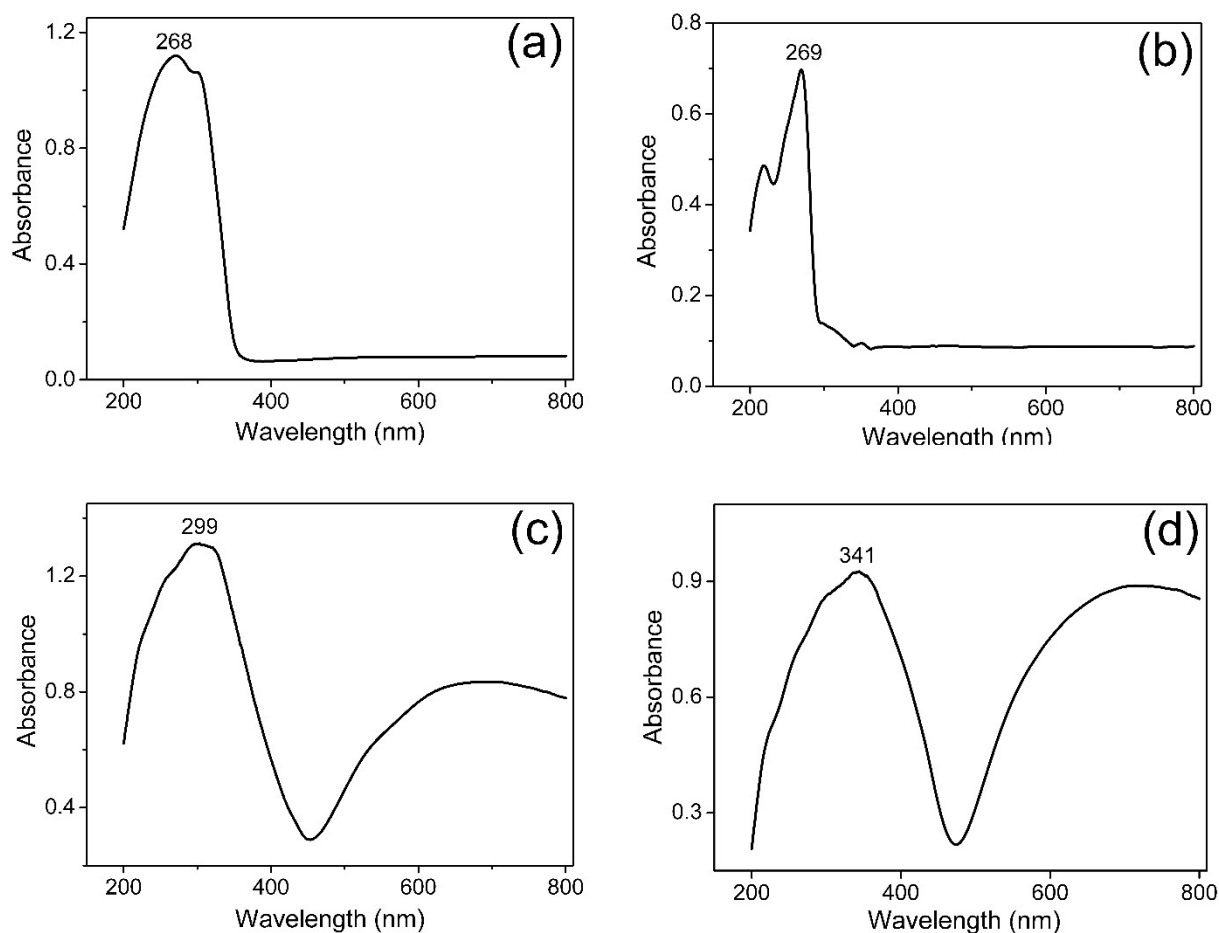


Fig. S10 (a-d) UV-vis diffuse reflectance spectra of bipy, PhPO_3H_2 , compounds **1** and **2**, respectively

5. Enzyme immobilization and characterization

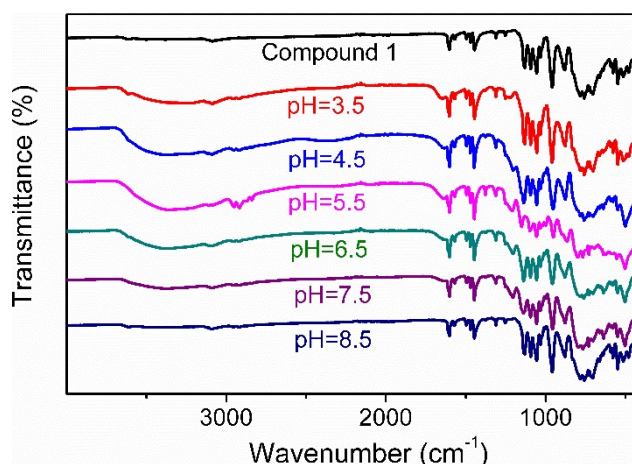


Fig. S11 FTIR spectra of compound **1** before (crystalline sample) and after (solid powders) soaking in PBS at pH 3.5–8.5 for 24 h

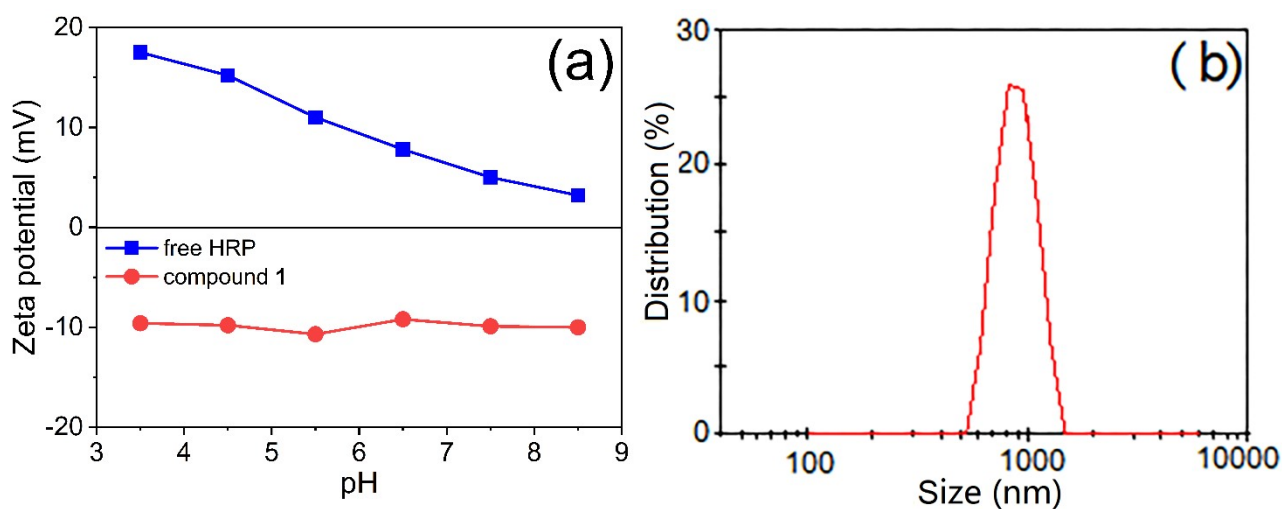
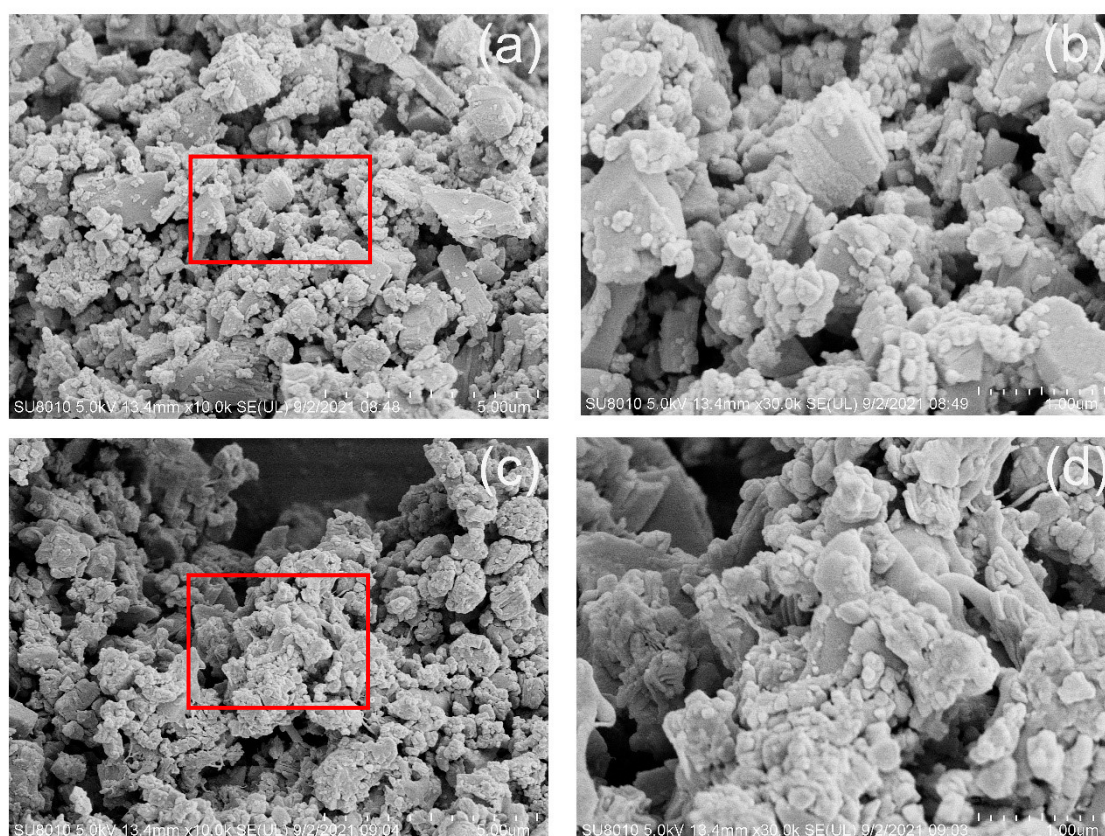


Fig. S12 (a) Surface zeta potential of free HRP and compound **1** (solid powders) at different pH. (b) The particle size distribution curve of grinded compound **1** powders

Before zeta potential measurement, the grinded compound **1** powder was dispersed in PBS, and then sonicated 15 min to form a uniform suspension with concentration of 0.5 mg mL⁻¹. As for free HRP, 1.6 mg mL⁻¹ of enzyme solution was applied to determine the zeta potential.

Table S4 The comparison of enzyme loading capacity for different support materials

Entry	Support material	Enzyme loading amount (mg g ⁻¹)	References
1	$\{[\text{Cu}(\text{H}_2\text{biim})_2][\{\text{Cu}(\text{H}_2\text{biim})_2(\mu\text{-H}_2\text{O})\}_2\text{Cu}(\text{H}_2\text{biim})(\text{H}_2\text{O})_2]\text{H}[\{\{\text{Cu}(\text{H}_2\text{biim})(\text{H}_2\text{O})_2\}_{0.5}\}_2(\mu\text{-C}_3\text{HN}_2\text{Cl}_2)\{\text{Cu}(\text{H}_2\text{biim})\}_2]\{\text{Z}(\text{H}_2\text{O})\text{P}_5\text{W}_{30}\text{O}_{110}\}]\cdot x\text{H}_2\text{O}\}_n$	157.5–158.7	26
2	$[(\text{TM}(\text{H}_2\text{biim})_2)_2(\text{C}_6\text{H}_5\text{PO}_3)_2\text{Mo}_5\text{O}_{15}]\cdot\text{H}_2\text{O}$	95.5–101.7	27
3	$[\text{Cu}_2\text{Mo}_6\text{O}_{20}(\text{C}_6\text{H}_6\text{N}_4)_2(\text{H}_2\text{O})_2]_n$	300.1	28
4	$\{[\text{Zn}(\text{H}_2\text{biim})_2]_3(\text{P}_2\text{W}_{18}\text{O}_{62})\}\cdot 6\text{H}_2\text{O}\}_n$	90.1	29
5	graphene oxide	100	13
6	layered double hydroxides (LDHs)	0.32	14
7	tyrosine-bridged periodic mesoporous organosilica	2.2	41
8	phosphorus-modified MCM-41	154	42
9	$\{((\text{Cu}(\text{bipy}))_2(\mu\text{-PhPO}_3)_2\text{Cu}(\text{bipy}))_2\text{H}(\text{PCuW}_{11}\text{O}_{39})\cdot 3\text{H}_2\text{O}\}_n$	268	This work

**Fig. S13** SEM images of (a, b) grinded compound **1** powders and (c, d) HRP/**1**. b and d are the magnified picture of square area in a and c, respectively

6. Degradation of phenolic compounds by HRP/1

(1) Determination of phenolic compound concentration

The concentration of residual phenolic compound can be determined as follows: 0.20 mL of the degraded solution was diluted to 1.80 mL with PBS (pH 3.5–8.5), and then mixed with 0.30 mL of 16.68 mmol L⁻¹ K₃Fe(CN)₆ in 0.25 mol L⁻¹ NaHCO₃, as well as 0.30 mL of 4.16 mmol L⁻¹ 4-AAP in 0.25 mol L⁻¹ NaHCO₃. The mixed solution was reacted for 5 min at room temperature and monitored the absorbance (506 nm) by UV-vis spectrophotometer (Fig. S3, ESI†).

(2) The degradative activity of HRP/1 towards different phenolic compounds

Table S5 The comparison of phenolic pollutant removal efficiency for various immobilized enzyme

Entry	Enzyme	Support material	Pollutants/Concentration (mg L ⁻¹)	Reaction time	Removal efficiency (%)	References
1	HRP	{((Cu(bipy)) ₂ (μ-PhPO ₃) ₂ Cu(bipy)) ₂ H (PCuW ₁₁ O ₃₉)·3H ₂ O} _n	Phenol/400	30 min	90.5 (TOC: 73.6)	This work ^a
			2,4-DCP/400		96.9 (TOC: 78.3)	
			4-CP/400		97.0 (TOC: 75.2)	
2	HRP	Polyacrylonitrile-based beads	2,4-DCP/282	12 h	90.0	45
3	HRP	Carbon nanospheres	Phenol/94	90 min	43.1	46
			2,4-DCP/94		95.0	
4	HRP	layered double hydroxides	Phenol/25	7 h	25	14
			Phenol/10		89.5	
5	Laccase	Heterophase TiO ₂ microspheres	2,4-DCP/10	3.5 h	85.9	47 ^c
6	RSVNP-CLEAs ^d	—	Phenol/100	1 h	92 (TOC: 78)	2

^aReaction conditions: 5.0 mg HRP/1 (268 mg g⁻¹), H₂O₂/phenol molar ratio of 2.3: 1, pH 7.5, reaction time of 30 min and temperature of 25 °C

^{b, c}Photo-enzyme integrated catalysis process

^dRSVNP: peroxidase isolated from *Raphanus sativus* var. *niger*; RSVNP-CLEAs: RSVNP was immobilized as a cross-linked enzyme aggregate (CLEAs)

(3) The effect of H₂O₂ on degradation of phenol in absence of catalyst

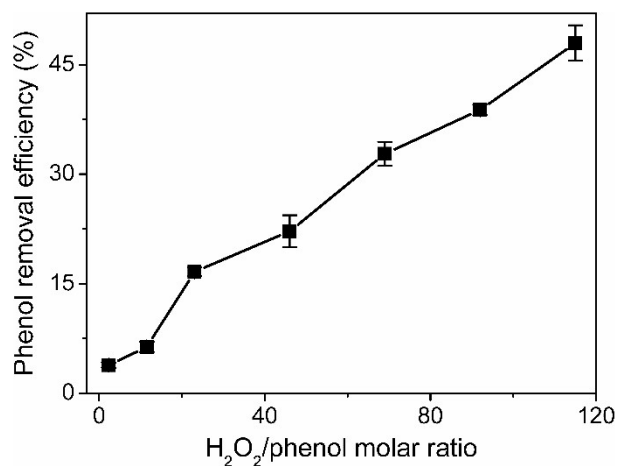


Fig. S14 Influence of H₂O₂ initial concentration on degradation of phenol (10 mL, 400 mg L⁻¹) without catalyst at pH 7.5. The amounts of fresh 30% H₂O₂ are 10, 50, 100, 200, 300, 400 and 500 μ L, that is, the final H₂O₂ concentrations in the reaction solution are about 9.8, 48.7, 97.0, 192.0, 285.3, 376.7 and 466.4 mmol L⁻¹ ($n(\text{H}_2\text{O}_2/\text{phenol}) = 2.3: 1, 11.5: 1, 23: 1, 46: 1, 69: 1, 92: 1, 115: 1$), respectively. Reaction time, 30 min